

# [Me<sub>2</sub>C(η<sup>5</sup>-C<sub>5</sub>H<sub>4</sub>)<sub>2</sub>Mdmit]<sub>2</sub>[TCNQF<sub>4</sub>] (M = Mo or W): Unprecedented Stoichiometry and Solid-State Arrangement in Charge-Transfer Salts of *ansa*-Metallocene Dithiolene Complexes

Isabelle V. Jourdain,<sup>†</sup> Marc Fourmigué,<sup>‡</sup> Fabrice Guyon,<sup>\*,†</sup> and  
Jacques Amaudrut<sup>†</sup>

Laboratoire de Chimie et Electrochimie Moléculaire, UFR des Sciences et Techniques,  
25030 Besançon Cedex, France, and Institut des Matériaux de Nantes (IMN),  
UMR 6502 CNRS–Université de Nantes, 2 rue de la Houssinière, BP 32229,  
44322 Nantes Cedex 03, France

Received November 6, 1998

The new *ansa* compounds Me<sub>2</sub>C(η<sup>5</sup>-C<sub>5</sub>H<sub>4</sub>)<sub>2</sub>Mdmit (M = Mo or W; dmit<sup>2-</sup> = 4,5-disulfanyl-1,3-dithiole-2-thionate) have been synthesized, and their oxidation by TCNQF<sub>4</sub> (perfluoro-7,7,8,8-tetracyano-*p*-quinodimethane) has been investigated. This reaction leads to two isostructural salts which surprisingly analyze as [Me<sub>2</sub>C(η<sup>5</sup>-C<sub>5</sub>H<sub>4</sub>)<sub>2</sub>Mdmit]<sub>2</sub>[TCNQF<sub>4</sub>] (M = Mo or W). Their structures exhibit an unprecedented organization of the TCNQF<sub>4</sub> moieties which are not dimerized as always observed in TCNQF<sub>4</sub> metallocenium charge-transfer salts. Both neutral and cationic organometallic species are present in the solid, in which layers are identified.

## Introduction

Elaboration of molecular solids exhibiting high electrical conductivity or bulk ferromagnetic or antiferromagnetic properties has been of great interest during the past 15 years and has led to the development of diverse strategies.<sup>1</sup> For our part, we have been interested in the preparation and study of paramagnetic dithiolene metallocene species. Recently we reported on the presence of strong antiferromagnetic interactions in [(Cp)<sub>2</sub>Mdddt]<sup>+</sup>[TCNQ]<sup>-</sup> (M = Mo or W, dddt<sup>2-</sup> = 5,6-dihydro-1,4-dithiine-2,3-dithiolate, and TCNQ = tetracyano-*p*-quinodimethane).<sup>2</sup> However, according to the presence of the bulky TCNQ<sup>-</sup> counteranions, the open-shell complexes mostly interact within layers, preventing the setting of an ordered three-dimensional ground state. We have shown that the nature and the dimensionality of the electronic interactions in the solid state are closely controlled by the shape and the composition of the molecules, as for example the Mo vs W substitution and the Se vs S vs O substitution in the dithiolene ligand.<sup>3</sup> In that respect, it was tempting to introduce other structural modification as a bridge between the two cyclopentadienyl ligands. Much work has been

devoted to the modification of the electronic properties, the structural features, and the reactivities imparted by the restricted geometry of the cyclopentadienyl rings in such *ansa*-metallocenes. Most of the investigations concern the chemistry of group 4 metals<sup>4</sup> in relation to homogeneous catalytic reactions, especially Ziegler–Natta type polymerization.<sup>5</sup> Nevertheless the synthesis of other metal complexes containing bridged cyclopentadienyl has also been achieved, and Green recently described the preparation of the group 6 compounds Me<sub>2</sub>C(η<sup>5</sup>-C<sub>5</sub>H<sub>4</sub>)<sub>2</sub>MCl<sub>2</sub> (M = Mo or W),<sup>6</sup> very attractive synthons to realize our goal. This paper reports on our first studies in the preparation of mixed dithiolene/*ansa*-molybdenocene or -tungstenocene paramagnetic species. The work was carried out with the dmit<sup>2-</sup> (dmit<sup>2-</sup> = 4,5-disulfanyl-1,3-dithiole-2-thionate) ligand<sup>7</sup> owing to its ability to develop a network of intermolecular interactions through short S–S contacts.<sup>8</sup>

## Results and Discussion

**Synthesis.** The reaction of [Me<sub>2</sub>C(η<sup>5</sup>-C<sub>5</sub>H<sub>4</sub>)<sub>2</sub>MCl<sub>2</sub>] (M = Mo or W) with Na<sub>2</sub>dmit in EtOH yields the corresponding air stable *ansa*-metallocene dithiolene complexes (M = Mo **1** and M = W **2**) with accompanying loss of NaCl (Scheme 1).

<sup>†</sup> UFR des Sciences et Techniques.

<sup>‡</sup> Université de Nantes.

(1) For example see: (a) The proceedings of the Fourth International Conference on Molecule-Based Magnets. Miller, J. S.; Epstein, A. J., Eds.; *Mol. Cryst. Liq. Cryst.* **1994**, 271–274. (b) Proceedings of the International Conference on Synthetic Metals. *Synth. Met.* **1995**, 71. (c) Williams, J. M.; Ferraro, J. R.; Thorn, R. J.; Carlson, K. D.; Geiser, U.; Wang, H. H.; Kini, A. M.; Whangbo, M. H. *Organic Superconductors (including Fullerenes)*; Prentice Hall: Englewood Cliffs, NJ, 1992.

(2) (a) Fourmigué, M.; Lenoir, C.; Coulon, C.; Guyon, F.; Amaudrut, J. *Inorg. Chem.* **1995**, 34, 4979–4985. (b) Jourdain, I. V.; Fourmigué, M.; Guyon, F.; Amaudrut, J. *J. Chem. Soc., Dalton Trans.* **1998**, 483–488.

(3) Fourmigué, M.; Domercq, B.; Jourdain, I.; Molinié, P.; Guyon, F.; Amaudrut, J. *Chem. Eur. J.* **1998**, 4, 1714–1723.

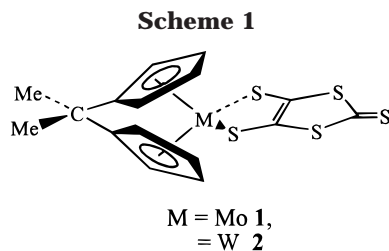
(4) (a) *Comprehensive Organometallic Chemistry II*; Abel, E. W., Stone G. A., Wilkinson, G., Eds.; Pergamon Press: Oxford, U.K., 1995; Vol. 4. (b) Halterman R. L. *Chem. Rev.* **1992**, 92, 965–994.

(5) (a) Rieger, B.; Jany, G.; Fawzi, R.; Steinmann, M. *Organometallics* **1994**, 13, 647–653. (b) Brintzinger, H. H.; Fischer, D.; Mülhaupt, R.; Rieger, B.; Waymouth, R. M. *Angew. Chem., Int. Ed. Engl.* **1995**, 34, 1143–1170.

(6) Labella, L.; Chernega, A.; Green, M. L. H. *J. Chem. Soc., Dalton Trans.* **1995**, 395–402.

(7) Varma, K. S.; Bury, A.; Harris, N. J.; Underhill, A. *Synthesis* **1987**, 737–738.

(8) Brousseau, M.; Valade, L.; Legros, J. P.; Cassoux, P.; Garbouskas, M.; Interrante, L. V. *J. Am. Chem. Soc.* **1986**, 108, 1908–1916.



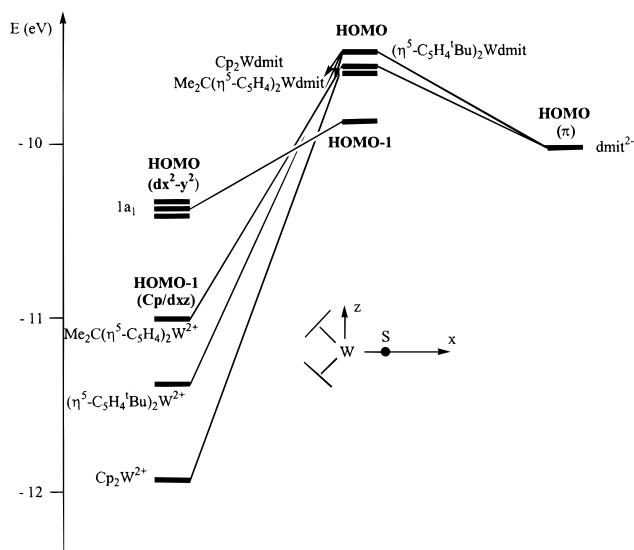
**Table 1. Electrochemical Data (in V vs Ag-0.1 mol dm<sup>-3</sup> AgClO<sub>4</sub>)**

complex	$E_{1/2}([M]^{+}/[M])$	$E_{1/2}([M]^{2+}/[M]^{+})$	ref
(Cp) <sub>2</sub> Modmit	-0.01	0.57	2a
(Cp) <sub>2</sub> Wdmit	-0.06	0.42	2b
( $\eta^5$ -C <sub>5</sub> H <sub>4</sub> <sup>t</sup> Bu) <sub>2</sub> Modmit	-0.04	0.53	9
( $\eta^5$ -C <sub>5</sub> H <sub>4</sub> <sup>t</sup> Bu) <sub>2</sub> Wdmit	-0.05	0.46	2b
( $\eta^5$ -C <sub>5</sub> H <sub>4</sub> SiMe <sub>3</sub> ) <sub>2</sub> Modmit	-0.04	0.56	9
( $\eta^5$ -C <sub>5</sub> H <sub>4</sub> SiMe <sub>3</sub> ) <sub>2</sub> Wdmit	-0.03	0.50	2b
Me <sub>2</sub> C( $\eta^5$ -C <sub>5</sub> H <sub>4</sub> ) <sub>2</sub> Modmit ( <b>1</b> )	0.07	0.58	this work
Me <sub>2</sub> C( $\eta^5$ -C <sub>5</sub> H <sub>4</sub> ) <sub>2</sub> Wdmit ( <b>2</b> )	0.07	0.52	this work

These diamagnetic complexes, to our knowledge the first examples of dithiolene coordination on *ansa*-metallocenes, were identified by elemental analysis and <sup>1</sup>H NMR spectroscopy. Their redox properties were investigated by cyclic voltammetry experiments performed in MeCN solution. The electrochemical characterization shows two one-electron reversible waves in the anodic range. The results are similar to those obtained with the unbridged complexes.<sup>2</sup> However, compared with the  $\eta^5$ -C<sub>5</sub>H<sub>5</sub> or  $\eta^5$ -C<sub>5</sub>H<sub>4</sub>R (R = SiMe<sub>3</sub> or <sup>t</sup>Bu) derivatives, the redox potential of the first oxidation wave is shifted significantly toward more anodic potentials by approximately 0.1 V (Table 1).

To gain information about the electronic influence of the *ansa* part, extended-Hückel calculations were conducted with the dmit<sup>2-</sup> ligand coordinated on ( $\eta^5$ -C<sub>5</sub>H<sub>5</sub>)<sub>2</sub>W<sup>2+</sup>, ( $\eta^5$ -C<sub>5</sub>H<sub>4</sub>CMe<sub>3</sub>)<sub>2</sub>W<sup>2+</sup>, and Me<sub>2</sub>C( $\eta^5$ -C<sub>5</sub>H<sub>4</sub>)<sub>2</sub>W<sup>2+</sup>. The interaction diagrams obtained in the ideal C<sub>2v</sub> conformation are represented in Figure 1. The slightly antibonding HOMO is mainly of dithiolene character ( $\pi$ ) with a weak interaction with the HOMO-1 of the metallocene fragment of d<sub>xz</sub> and cyclopentadienyl (p<sub>z</sub>) characters, while the HOMO-1 consists almost exclusively of the d<sub>x<sup>2</sup>-y<sup>2</sup></sub> orbital of the metallocene fragment. Concerning the complexes, no significant differences in terms of energy are observed on going from substituted to unsubstituted cyclopentadienyl. The influence of the bridge lies principally in the energies of the HOMO-1 orbitals of the metallocene fragments. Indeed a difference of 1 eV is calculated between the HOMO-1 orbitals of Cp<sub>2</sub>W<sup>2+</sup> and Me<sub>2</sub>C( $\eta^5$ -C<sub>5</sub>H<sub>4</sub>)<sub>2</sub>W<sup>2+</sup>. Thus, the latter interacts more strongly with the HOMO of the dithiolene moiety since their energies are closest (Table 2).

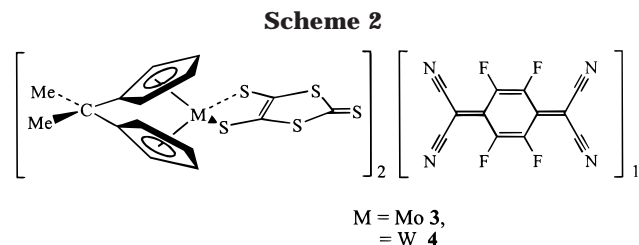
Given the electrochemical data, it can be concluded that the oxidation of both **1** and **2** also requires a strong oxidizer such as TCNQF<sub>4</sub> (perfluoro-7,7,8,8-tetracyano-p-quinodimethane:  $E_{1/2} = +0.07$  V vs Ag/Ag<sup>+</sup>) instead of TCNQ. Indeed treatment of an acetonitrile solution of TCNQF<sub>4</sub> with a ca. 1 molar equiv of **1** or **2** was found to afford a purple solution from which crystalline platelets of respectively [Me<sub>2</sub>C( $\eta^5$ -C<sub>5</sub>H<sub>4</sub>)<sub>2</sub>Modmit]<sub>2</sub>[TCNQF<sub>4</sub>] (**3**) or [Me<sub>2</sub>C( $\eta^5$ -C<sub>5</sub>H<sub>4</sub>)<sub>2</sub>Wdmit]<sub>2</sub>[TCNQF<sub>4</sub>] (**4**) could be isolated. The striking 2:1 stoichiometry, i.e., two organometallic donors for one TCNQF<sub>4</sub> acceptor,



**Figure 1.** Extended Hückel fragment orbital interactions of the Cp( $\eta$ )<sub>2</sub>Wdmit complexes in a C<sub>2v</sub> geometry.

**Table 2. Nature of the Molecular HOMO for the Cp( $\eta$ )<sub>2</sub>Wdmit Complexes**

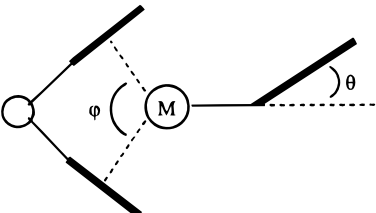
complex	% HOMO of the dmit <sup>2-</sup> fragment	% HOMO-1 of the Cp( $\eta$ ) <sub>2</sub> W <sup>2+</sup> fragment
Cp <sub>2</sub> Wdmit	86.3	10.2
( $\eta^5$ -C <sub>5</sub> H <sub>4</sub> CMe <sub>3</sub> ) <sub>2</sub> Wdmit	83	3.1
Me <sub>2</sub> C( $\eta^5$ -C <sub>5</sub> H <sub>4</sub> ) <sub>2</sub> Wdmit	77.5	15.2



was ascertained from the X-ray structural analysis and elemental analysis. Note also that a microcrystalline 1:1 salt was obtained upon mixing concentrated solutions of both components, while the 2:1 salt was obtained only from slow concentration of dilute solutions. The IR spectroscopic data for the two salts, especially the nitrile stretching frequencies (2175 and 2170 cm<sup>-1</sup> for **3** and 2193 and 2170 cm<sup>-1</sup> for **4**), point toward a charge transfer since these values are consistent with an anionic TCNQF<sub>4</sub><sup>•-</sup>.<sup>10,11</sup> The reduction of the organic acceptor is also supported by the UV-visible spectra of **3** and **4**, which exhibit a visible transition near 410 nm that is red shifted from the neutral TCNQF<sub>4</sub> transition reported at 390 nm. This is in agreement with the results reported by Miller and co-workers<sup>12</sup> on the electronic absorption spectra for [TCNQF<sub>4</sub>]<sup>n</sup> (n = 0, 1-, 2-) (Scheme 2).

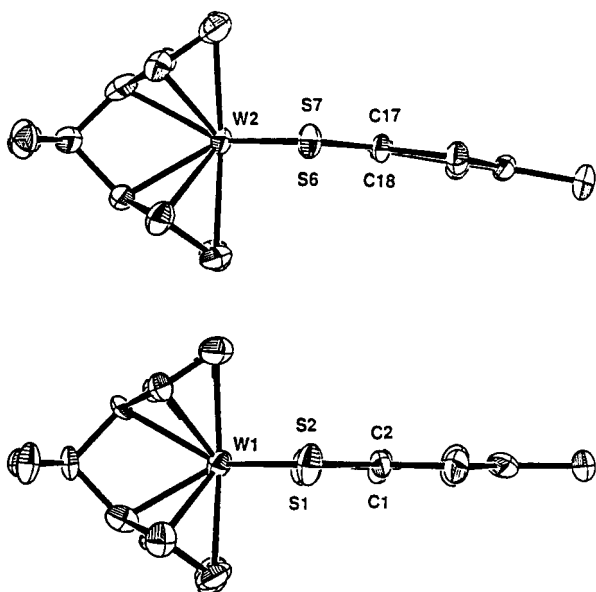
**Structural Analysis.** The two salts are isostructural and crystallize in the triclinic system, space group  $P\bar{1}$ . Therefore, only figures relative to **4** will be presented

- (9) Guyon, F. Ph.D. thesis, Université de Besançon, 1994.  
 (10) Emge, T. J.; Maxfield M.; Cowan D. O.; Kistenmach T. J. *Mol. Cryst. Liq. Cryst.* **1981**, *65*, 161-178.  
 (11) Miller, J. S.; Zang, J. H.; Reiff, W. M. *Inorg. Chem.* **1987**, *26*, 600.  
 (12) Dixon, D. A.; Calabrese, J. C.; Miller, J. S. *J. Phys. Chem.* **1989**, *93*, 2284-2291.

**Table 3. Selected Bonds (in Å) and Angles (deg) of Cp<sub>2</sub>Mdithiolene Complexes**


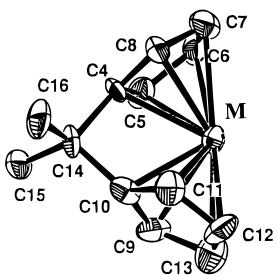
complex	M-S	C-S	C-C	$\theta^a$	$\varphi$	M-C max. and min	ref
[(Cp) <sub>2</sub> Modmit][TCNQF <sub>4</sub> ]	2.444(4)	1.684(13)	1.43(2)	10.2	136.38	2.393(15)	3
	2.448(4)	1.681(14)				2.291(14)	
[(Cp) <sub>2</sub> Wdmit][TCNQF <sub>4</sub> ]	2.426(2)	1.721(6)	1.374(8)	27.6	135.1	2.373(6)	3
	2.441(1)	1.722(6)				2.313(6)	
<b>3</b> (A)	2.450(2)	1.720(7)	1.367(9)	7.35	113.86	2.392(7)	this work
	2.454(2)	1.725(7)				2.222(6)	
<b>3</b> (B)	2.440(2)	1.760(8)	1.344(10)	0.68	115.16	2.447(2)	this work
	2.447(2)	1.731(8)				2.248(6)	
<b>4</b> (A)	2.444(3)	1.710(11)	1.38(2)	6.99	113.67	2.399(11)	this work
	2.443(3)	1.727(11)				2.235(11)	
<b>4</b> (B)	2.431(3)	1.743(14)	1.39(2)	0.29	113.79	2.396(14)	this work
	2.436(3)	1.740(13)				2.227(11)	

<sup>a</sup> Folding angle between S-M-S and dithiolene planes.



**Figure 2.** Eclipsed views of the two different organometallic molecules in the salt **4** (at the bottom molecule B and at the top molecule A).

in the discussion that follows. Molecules are located in general positions in the unit cell. Concerning the organometallic species, two crystallographically independent molecules are observed (A and B in Figure 2) which differ mainly by the folding of the MS<sub>2</sub>C<sub>2</sub> plane along the S-S axis (angle  $\theta$ ) and by the C-S and M-S bond lengths (Table 3). Earlier studies have shown a close correlation between the folding angle and the electronic structure of the metal.<sup>2,13</sup> Indeed, the value of  $\theta$  increases upon lowering the electronic count of the metal:  $\theta$  is close to 0° in the 18-electron d<sup>2</sup> complexes,<sup>2a</sup> while it amounts to 45–50° in the 16-electron d<sup>0</sup> complexes.<sup>14</sup> A tendency to fold is also observed in the intermediate paramagnetic d<sup>1</sup> complexes with  $\theta$  values

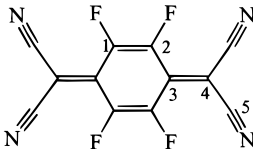
**Table 4. Selected Bond Distances (Å) in Me<sub>2</sub>C(C<sub>5</sub>H<sub>4</sub>)<sub>2</sub>M<sup>2+</sup> Fragment**


bond	(3) A	(3) B	(4) A	(4) B
M-C4	2.222(6)	2.250(6)	2.252(12)	2.255(10)
M-C5	2.258(7)	2.276(6)	2.281(12)	2.273(12)
M-C8	2.259(6)	2.264(7)	2.273(12)	2.292(11)
M-C6	2.390(7)	2.368(7)	2.396(12)	2.396(14)
M-C7	2.389(6)	2.343(8)	2.389(13)	2.379(13)
M-C10	2.241(6)	2.248(6)	2.235(11)	2.227(11)
M-C9	2.266(6)	2.269(7)	2.283(13)	2.263(12)
M-C11	2.274(7)	2.254(6)	2.255(12)	2.256(12)
M-C12	2.392(7)	2.386(7)	2.399(11)	2.358(14)
M-C13	2.380(6)	2.363(8)	2.393(13)	2.36(2)
C4-C5	1.430(9)	1.422(9)	1.49(2)	1.41(2)
C4-C8	1.405(8)	1.421(9)	1.41(2)	1.46(2)
C5-C6	1.408(10)	1.410(10)	1.40(2)	1.43(2)
C8-C7	1.410(9)	1.386(9)	1.44(2)	1.41(2)
C6-C7	1.401(11)	1.366(11)	1.38(2)	1.36(2)
C10-C9	1.419(9)	1.411(10)	1.43(2)	1.46(2)
C10-C11	1.423(10)	1.416(9)	1.43(2)	1.41(2)
C9-C13	1.410(10)	1.405(10)	1.41(2)	1.39(2)
C11-C12	1.424(9)	1.403(10)	1.42(2)	1.39(2)
C12-C13	1.395(10)	1.370(11)	1.40(2)	1.34(2)

between 0° and ca. 30° depending upon the nature of the metal, the dithiolene, and the counteranion.<sup>3</sup> In addition it is well established that upon oxidation the dithiolene ligand adopts a more dithioketonic structure with shorter C-S bonds and longer C-C bonds, as observed here for molecule A when compared with molecule B. From these data and the stoichiometry, we can conclude that both neutral (molecule B) and cationic (molecule A) species are present in the salts. Note also that the single *ansa*-bridging atom has introduced several distinct structural alterations. First of all, the small value of the angle ( $\varphi$ ) between the normal of the

(13) Lauher, J. W.; Hoffmann, R. *J. Am. Chem. Soc.* **1976**, *98*, 1729–1741.

(14) Guyon, F.; Lenoir, C.; Fourmigué, M.; Larsen, J.; Amaudrut, J. *Bull. Soc. Chim. Fr.* **1994**, *131*, 217–226.

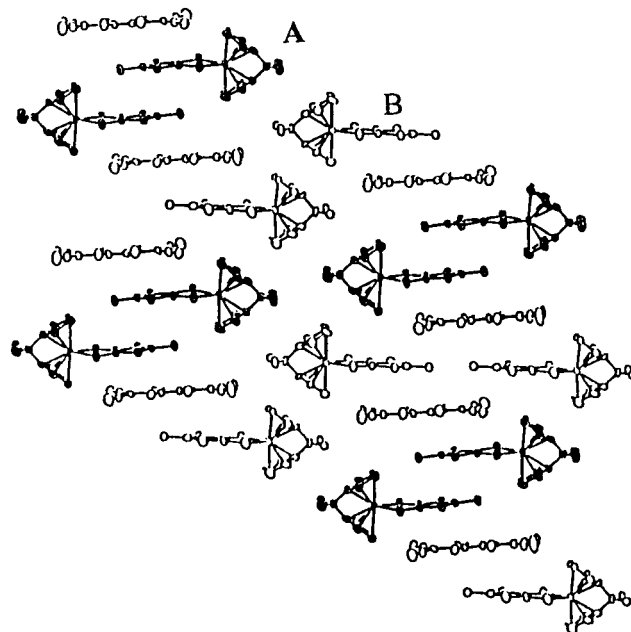
**Table 5. Experimental Geometric Parameters (in Å) and IR (C≡N) Stretching Frequencies for TCNQF<sub>4</sub>**


parameter	TCNQF <sub>4</sub> <sup>10</sup> (TCNQF <sub>4</sub> ) <sup>0</sup>	[(Cp) <sub>2</sub> W(dmit)][TCNQF <sub>4</sub> ] <sup>3</sup> (TCNQF <sub>4</sub> ) <sub>2</sub> <sup>2-</sup>	<b>3</b> (TCNQF <sub>4</sub> ) <sup>-</sup>	<b>4</b> (TCNQF <sub>4</sub> ) <sup>-</sup>	[Cp* <sub>2</sub> Fe] <sub>2</sub> [TCNQF <sub>4</sub> ] <sup>16</sup> (TCNQF <sub>4</sub> ) <sub>2</sub> <sup>2-</sup>
C <sub>1</sub> –C <sub>2</sub>	1.335	1.358(8)	1.343(9)	1.355(35)	1.373
C <sub>2</sub> –C <sub>3</sub>	1.439	1.420(8)	1.415(14)	1.42(2)	1.398
C <sub>3</sub> –C <sub>4</sub>	1.373	1.414(8)	1.401(9)	1.42(2)	1.457
C <sub>4</sub> –C <sub>5</sub>	1.440	1.42(1)	1.418(11)	1.407(22)	1.403
C <sub>5</sub> –N	1.142	1.14(1)	1.149(10)	1.14(2)	1.154
ν(C≡N), cm <sup>-1</sup>	2230, 2215	2194, 2179	2175, 2170	2193, 2170	2167, 2133

ring planes is indicative of the highly strained nature of this *ansa* system.<sup>15</sup> As a consequence of this stiffness, the M–C(Cp) bond distances lie in a broader range than in the unbridged complexes ( $\Delta d_{\max} = 0.2$  Å vs 0.1 Å) (Table 3). The M–C(*ipso*) bond is significantly shortened when compared to the M–C bonds of the non-*ansa* compounds. In addition the C<sub>6</sub>–C<sub>7</sub> and C<sub>12</sub>–C<sub>13</sub> bonds are consistently shorter than the remaining C–C bonds within the rings (Table 4). These distortions indicate that the interaction of [Me<sub>2</sub>C(η<sup>5</sup>-C<sub>5</sub>H<sub>4</sub>)<sub>2</sub>]<sup>2-</sup> with the metal contains a small contribution of η<sup>2</sup> and η<sup>3</sup> bonds.<sup>16</sup>

As expected, the bond lengths within the TCNQF<sub>4</sub> molecule point toward a reduced anion radical since it adopts a more benzenoid form than the neutral TCNQF<sub>4</sub> and dismiss the hypothesis of a TCNQF<sub>4</sub> dianion (Table 5). In addition the TCNQF<sub>4</sub> molecules in **3** and **4** have planar D<sub>2h</sub> symmetry, unlike the TCNQF<sub>4</sub> dianion, which is nonplanar. Compared with the situation encountered in TCNQF<sub>4</sub> salts of organometallic donors, structural analysis of **3** and **4** reveals an unprecedented organization of the TCNQF<sub>4</sub> moieties (Figure 3). Indeed, the TCNQF<sub>4</sub> molecules are isolated from each other, while they usually organize into dimeric dianionic moieties.<sup>17</sup> Note also that the bond lengths within this isolated radical are intermediate between those of the neutral molecule and those of the dimeric dianionic species (Table 5).

From the analysis of the shortest intermolecular contacts we can identify layers in the solid (Figure 4) which result from face-to-face arrangement between the dithiolene part and the planar TCNQF<sub>4</sub> molecules (Figure 3). The oxidized molecules A arrange into centrosymmetrical dimers, a common feature in the [Cp<sub>2</sub>M(dithiolene)]<sup>+</sup> salts. However the relative orientation of the molecules depends strongly upon the nature of the dithiolene and the cyclopentadienyl ligands. In those structures the two dmit<sup>2-</sup> ligands fit tightly into each other by positioning the terminal sulfur above the carbon–carbon bond (Figure 5). The plane-to-plane distances are the same in the two compounds **3** and **4**

**Figure 3.** Arrangement of the molecules within a layer in [Me<sub>2</sub>C(η<sup>5</sup>-C<sub>5</sub>H<sub>4</sub>)<sub>2</sub>Wdmit]<sub>2</sub>[TCNQF<sub>4</sub>], **4**.

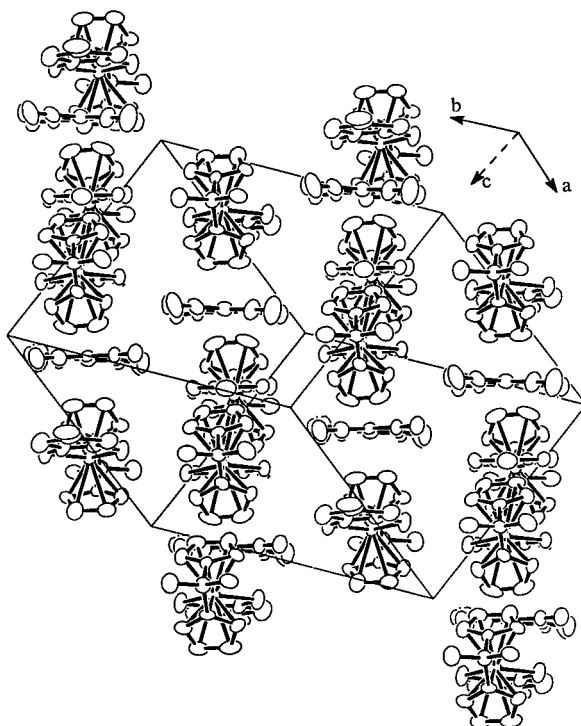
(3.66 Å). No intermolecular distances lower than twice the sum of the sulfur van der Waals radius are identified. This weak overlap within the dimers is confirmed by the extended Hückel calculations of the HOMO–HOMO interaction energies, which afford values lower than 20 meV in the two salts.<sup>18</sup> These dimers are located between two parallel anionic TCNQF<sub>4</sub><sup>-</sup>, giving rise to tetramolecular moieties (TCNQF<sub>4</sub><sup>-</sup>/A<sup>•+</sup>/A<sup>•+</sup>/TCNQF<sub>4</sub><sup>-</sup>) separated from each other by a neutral organometallic molecule B (Figure 3 and [101] direction in Figure 4). Within this tetramolecular unit, the dithiolene and the TCNQF<sub>4</sub> mean planes are not fully parallel (the dihedral angles amount to 5.04° and 4.65° in the Mo and W salts, respectively) and adopt a face-to-face arrangement where the exocyclic carbon–sulfur bond is positioned above the quinone cycle (Figure 6). Several short contacts between these species are observed (C<sub>C=C</sub>⋯C<sub>C=N</sub> = 3.261 Å (M = Mo and W); S<sub>C=S</sub>⋯C<sub>ring</sub> = 3.442 Å (M = Mo), 3.418 Å (M = W)). But this overlap interaction cannot be more closely evaluated due to the inability of the extended Hückel calculations to evaluate quantita-

(15) (a) Labella, L.; Chernaga, A.; Green, M. L. H. *J. Organomet. Chem.* **1995**, 485, C18–21. (b) Shaltout, R. M.; Corey, J. Y. *Tetrahedron* **1995**, 51, 4309–4320.

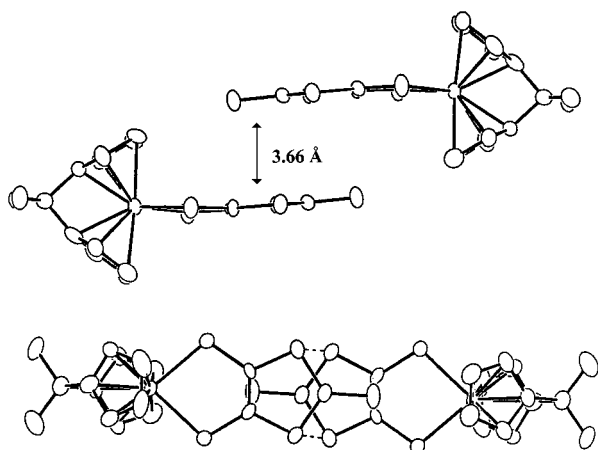
(16) (a) Smith, J. A.; von Seyerl, J.; Huttner, G.; Brintzinger, H. H. *J. Organomet. Chem.* **1979**, 173, 175. (b) Bajgur, C. S.; Tikkanen, W. R.; Petersen, J. *Inorg. Chem.* **1985**, 24, 2539–2546.

(17) This list is meant to be representative and not exhaustive: (a) Ward, M. D.; Johnson, D. C. *Inorg. Chem.* **1987**, 26, 4213. (b) Miller, J. S.; Zhang, J. H.; Reiff, W. M. *Inorg. Chem.* **1987**, 26, 600. (c) Wiygul, F. M.; Emge, T. J.; Kistenmacher, T. J. *Mol. Cryst. Liq. Cryst.* **1982**, 77, 6203.

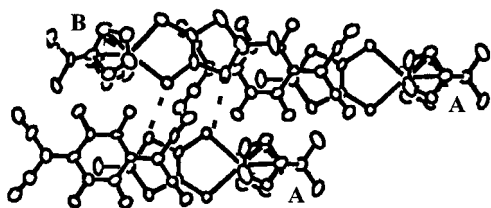
(18) These values were found by calculating the energy difference between the highest occupied molecular orbital (HOMO) and the lowest unoccupied molecular orbital (LUMO) of the dimeric [Me<sub>2</sub>C(η<sup>5</sup>-C<sub>5</sub>H<sub>4</sub>)<sub>2</sub>Mdmit]<sub>2</sub><sup>2+</sup> moieties.



**Figure 4.** Stacking of the species in the [101] direction in  $[\text{Me}_2\text{C}(\eta^5\text{-C}_5\text{H}_4)_2\text{Wdmit}]_2[\text{TCNQF}_4]$ , **4**.



**Figure 5.** Side view and top view (relative to the  $\text{dmit}^{2-}$  ligand) of the  $[\text{Me}_2\text{C}(\eta^5\text{-C}_5\text{H}_4)_2\text{Wdmit}]_2^{2+}$  dimer.



**Figure 6.** Top view of two adjacent layers (relative to the  $\text{dmit}^{2-}$  ligand). The short intermolecular contacts linking the layers are represented in dashed lines.

tively the interaction energy between two different species. Several short lateral intermolecular contacts have also been identified between the above-mentioned layers ( $S_A \cdots S_B = 3.242 \text{ \AA}$  ( $M = \text{Mo}$ ),  $3.244 \text{ \AA}$  ( $M = \text{W}$ ) (Figure 6);  $N \cdots C_{\text{Cp}} = 3.155 \text{ \AA}$  ( $M = \text{Mo}$ ),  $3.167 \text{ \AA}$  ( $M = \text{W}$ )).

The magnetic susceptibility has been measured in the temperature range 5–300 K for both salts. The experi-

mental data are well simulated with the sum of a diamagnetic term and a Curie–Weiss law ( $\chi = C(T - \theta)^{-1}$ ) with a  $C$  value of 0.0137 (**3**) and 0.0031 (**4**) indicating ca. 0.03 and 0.01 spin per molecule, respectively. This essentially diamagnetic behavior, observed here in both the molybdenum and the tungsten salts, is in apparent contradiction with the convincing experimental evidence (IR, UV–visible, bond lengths) for the presence of anionic  $\text{TCNQF}_4^{•-}$  and monocationic radical species and can only be attributed to a pairing of those radical species. The weak dithiolene/dithiolene interaction cannot be held responsible for a cation radical/cation radical pairing within the tetramer and will also allow the two  $\text{TCNQF}^{•-}$  to be unpaired, in contradiction with the observed diamagnetism. On the other hand, the short contacts identified between the organometallic cations and the  $\text{TCNQF}^{•-}$  anions within each tetramer could be at the origin of a donor/acceptor interaction.<sup>19</sup> Further investigations are in progress to rationalize the influence of the *ansa* part in these original properties.

## Experimental Section

**General Comments.** All reactions were carried out under an atmosphere of dry argon using standard Schlenk techniques. Solvents were purified by standard methods and freshly distilled under nitrogen. The compounds  $[\text{Me}_2\text{C}(\eta^5\text{-C}_5\text{H}_4)_2\text{MCl}_2]$  ( $M = \text{Mo}$  or  $\text{W}$ ) were prepared according to the literature method.<sup>6</sup> The method described by Wheland and Martin was employed for the synthesis of  $\text{TCNQF}_4$ .<sup>20</sup> The NMR spectra were recorded on a 200 MHz Bruker spectrometer in  $\text{CDCl}_3$  with  $\text{SiMe}_4$  as the internal references. Magnetic susceptibility data were collected on a commercial Quantum Design MPMS5 SQUID susceptometer. Data were corrected for molecular diamagnetism and holder contributions. Elemental analyses were performed at the Service Central d'Analyse, CNRS, Vernaison, France.

**Electrochemical Measurements.** Cyclic voltammetry experiments were performed with a Radiometer PGP 201 potentiostat. The electrolyte consisted of 0.1  $\text{MN}^+\text{Bu}_4\text{PF}_6$  solution in acetonitrile dried on molecular sieves. A three-compartment cell was used with a platinum working electrode (diameter 2 mm), a platinum counter electrode, and an  $\text{Ag-0.1 mol dm}^{-3} \text{AgClO}_4$  reference electrode. Experiments were performed under argon flow. After each measurement the reference electrode was checked against the ferrocene–ferrocinium couple (+0.025 V).

**Synthesis of  $[\text{Me}_2\text{C}(\eta^5\text{-C}_5\text{H}_4)_2\text{Modmit}]$ , **1**.** Equimolar quantities (1 mmol) of  $[\text{Me}_2\text{C}(\eta^5\text{-C}_5\text{H}_4)_2\text{MoCl}_2]$  and  $\text{Na}_2\text{dmit}^{2-}$  were refluxed in EtOH (50  $\text{cm}^3$ ) overnight under argon. After filtration, the red solution was removed under reduced pressure and the residue was extracted with  $\text{CHCl}_3$ . Concentration followed by chromatography [ $\text{SiO}_2$ ,  $\text{CHCl}_3$ , then  $\text{CH}_2\text{Cl}_2$ ] afforded the complex  $[\text{Me}_2\text{C}(\eta^5\text{-C}_5\text{H}_4)_2\text{Modmit}]$  as a red powder (0.115 g, 25%). IR (KBr): 1054 ( $\nu_{\text{C-S}}$ ).  $^1\text{H NMR}$  (200 MHz,  $\text{CDCl}_3$ ):  $\delta$  1.14 (s, 6H,  $\text{CMe}_2$ ), 5.23 (4H) and 5.52 (4H) (m,  $(\text{C}_5\text{H}_4)_2(u\text{-CMe}_2)$ ). Anal. Calcd for  $\text{C}_{16}\text{H}_{14}\text{MoS}_5$ : C, 41.56; H, 3.03; S, 34.64. Found: C, 41.59; H, 3.14; S, 33.58. UV–visible ( $\text{CH}_3\text{CN}$ ) [ $\lambda_{\text{max}}$ , nm ( $\epsilon$ ): 497 (21000)].

**Synthesis of  $[\text{Me}_2\text{C}(\eta^5\text{-C}_5\text{H}_4)_2\text{Wdmit}]$ , **2**.** This was carried out in a manner similar to the synthesis of **1** from  $[\text{Me}_2\text{C}(\eta^5\text{-C}_5\text{H}_4)_2\text{WCl}_2]$  (1 mmol) and  $\text{Na}_2\text{dmit}$  (1 mmol). Yield: (0.110 g, 20%). IR (KBr): 1053.8 ( $\nu_{\text{C-S}}$ ).  $^1\text{H NMR}$  (200 MHz,  $\text{CDCl}_3$ ):  $\delta$

(19) Extended Hückel calculations cannot be used here for evaluating such a donor–acceptor interaction which involve two different molecules whose frontiers orbital energies would depend of the orbital types involved in the calculations. Such calculations are restricted indeed to homodimers.

(20) Wheland, R. C.; Martin, E. L. *J. Org. Chem.* **1975**, *40*, 3101.

Table 6. Crystallographic Data

	3	4
formula	C <sub>44</sub> H <sub>28</sub> F <sub>4</sub> N <sub>4</sub> S <sub>10</sub> Mo <sub>2</sub>	C <sub>44</sub> H <sub>28</sub> F <sub>4</sub> N <sub>4</sub> S <sub>10</sub> W <sub>2</sub>
fw	1201.18	1377
color, habit	black, plate	
cryst size (mm)	0.135 × 0.077 × 0.008	0.21 × 0.17 × 0.03
T (K)	293(2)	293(2)
cryst syst	triclinic	triclinic
space group	P1	P1
a (Å)	12.394(14)	12.3850(14)
b (Å)	13.7418(14)	13.7614(13)
c (Å)	14.121(2)	14.115(2)
α (deg)	92.115(14)	92.096(12)
β (deg)	102.432(15)	102.433(12)
γ (deg)	108.201(14)	108.117(11)
V (Å <sup>3</sup> )	2217.0(5)	2218.9(4)
Z	2	2
ρ calc (g cm <sup>-3</sup> )	1.799	2.061
μ (mm <sup>-1</sup> )	1.094	5.708
F(000)	1200	1328
λ (Å)	0.710 73	0.710 73
2θ range, deg	1.57–24.02	1.78–24.03
index ranges	−14 ≤ h ≤ 14, −15 ≤ k ≤ 15, −16 ≤ l ≤ 16	−14 ≤ h ≤ 14, −14 ≤ k ≤ 14, −16 ≤ l ≤ 16
no. of collected reflns	17 634	18 383
no. of ind reflns	6519	6541
largest diff peak and hole, e Å <sup>-3</sup>	0.416 and −0.491	0.967 and −1.299
final R indices	R1 = 0.0398, wR2 = 0.0537	R1 = 0.0370, wR2 = 0.0555
R indices	R1 = 0.1028, wR2 = 0.0636	R1 = 0.0911, wR2 = 0.0664
GOF on F <sup>2</sup>	0.745	0.776

$$^a R(F) = \frac{\sum ||F_o| - |F_c||}{\sum F_o}, \quad ^b wR(F) = \frac{[\sum [w(F_o^2 - F_c^2)^2]}{\sum [w(F_o^2)]^2}]^{1/2}.$$

1.09 (s, 6H, CMe<sub>2</sub>), 5.35 (4H) and 5.39 (4H) (m, (C<sub>5</sub>H<sub>4</sub>)<sub>2</sub>(μ-CMe<sub>2</sub>)). Anal. Calcd for C<sub>16</sub>H<sub>14</sub>WS<sub>5</sub>: C, 34.92; H, 2.55; S, 29.10. Found: C, 34.76; H, 2.62; S, 28.66. UV–visible (CH<sub>3</sub>CN) [λ<sub>max</sub>, nm (ε)]: 496 (7900).

**Synthesis of the TCNQF<sub>4</sub> Charge-Transfer Salts.** These salts were prepared by mixing hot solutions of TCNQF<sub>4</sub> (0.1

mmol) dissolved in dry CH<sub>3</sub>CN (20 cm<sup>3</sup>) and the dithiolene complex (0.1 mmol) dissolved in CH<sub>2</sub>Cl<sub>2</sub> (15 cm<sup>3</sup>). Slow concentration and cooling of the resulting dark solutions afforded crystalline platelets of the title compounds. [Me<sub>2</sub>C(η<sup>5</sup>-C<sub>5</sub>H<sub>4</sub>)<sub>2</sub>Modmit]<sub>2</sub>[TCNQF<sub>4</sub>], **3** Anal. Calcd for C<sub>44</sub>F<sub>4</sub>H<sub>28</sub>N<sub>4</sub>S<sub>10</sub>Mo<sub>2</sub>: C, 44.00; H, 2.33; N, 4.67; S, 26.67. Found: C, 44.28; H, 2.38; N, 4.56; S, 25.64. UV–visible (CH<sub>3</sub>CN) [λ<sub>max</sub>, nm (ε)]: 410 (80000). [Me<sub>2</sub>C(η<sup>5</sup>-C<sub>5</sub>H<sub>4</sub>)<sub>2</sub>Wdmit]<sub>2</sub>[TCNQF<sub>4</sub>], **4**. Anal. Calcd for C<sub>44</sub>F<sub>4</sub>H<sub>28</sub>N<sub>4</sub>S<sub>10</sub>W<sub>2</sub>: C, 38.38; H, 2.05; N, 4.07; S, 23.28. Found: C, 38.38; H, 2.05; N, 3.94; S, 22.89. UV–visible (CH<sub>3</sub>CN) [λ<sub>max</sub>, nm (ε)]: 410 (85000).

**Crystallographic Data Collection and Structure Determination for 3 and 4.** Crystals were mounted in glass capillaries using Araldite glue. Data were collected on a Stoe-IPDS diffractometer, with graphite-monochromated Mo Kα radiation (λ 0.710 73 Å). Details are given in Table 6. Numerical absorption correction was applied (FACEIT, Stoe). The structure was solved by direct methods and refined anisotropically by full-matrix least-squares on F<sup>2</sup> (program SHELXTL 5.04<sup>21</sup>). Hydrogen atoms were placed in calculated positions (C–H 0.93 Å), included in structure-factor calculations but not refined.

**Extended Hückel Calculations.** Extended-Hückel type calculations<sup>22</sup> were performed with double-ζ quality orbitals<sup>23</sup> for C, W, F, N, and S. Single-ζ orbitals were used for H.

**Supporting Information Available:** Complete tables of atomic coordinates, H atom parameters, bond distances, bond angles, and isotropic thermal parameters. This material is available free of charge via the Internet at <http://pubs.acs.org>.

OM980910D

(21) Sheldrick, G. M. *SHELXTL*, version 5; Siemens Analytical X-Ray Division: Madison, WI, 1994.

(22) Hoffmann, R. *J. Chem. Phys.* **1963**, *39*, 1397.

(23) (a) Whangbo, M.-H.; Williams, J. M.; Leung, P. C. W.; Beno, M. A.; Emge, T. J.; Wang, H. H.; Carlson, K. D.; Crabtree, G. W. *J. Am. Chem. Soc.* **1985**, *105*, 5815. (b) Clementi, E.; Roetti, C. *At. Nucl. Data Tables* **1974**, *14*, 177.